Application of Finite Elements Method for Improvement of Acoustic Emission Testing

S Gerasimov[1], **T Sych**[2] **and V Kuleshov**[3]

[1] Professor of Department of Structural Mechanics, Siberian Transport University, Novosibirsk, Russia
[2] PhD Student of Department of Structural Mechanics, Siberian Transport University, Novosibirsk, Russia
[3] Professor of Institute of Non-Destructive Testing, Tomsk Polytechnic University, Tomsk, Russia
E-mail: 912267@gmail.com

Abstract. The paper deals with the acoustic emission sensor modeling by means of FEM system COSMOS/M. The following types of acoustic waves in the acoustic emission sensors are investigated: the longitudinal wave and transversal wave. As a material is used piezoelectric ceramics. The computed displacements are compared with physical model under consideration. The results of numerical and physical simulations of the processes of acoustic wave propagation in solebar of the freight-car truck are presented. The fields of dynamic displacements and stresses were calculated for improvement of acoustic emission testing method.

1. Introduction

The acoustic emission (AE) technology is widely used in field testing of high-pressure vessels, pipelines and castings. The AE-sensor constitutes the first part in an AE measurement chain and as of this is of particular importance [1]. A subsequent measurement system can only process signals which the AE-sensor picked up. An AE-sensor converts the surface movement caused by an elastic wave into an electrical signal which can be processed by the measurement equipment. The piezoelectric element of the AE-sensor should pick up faintest surface movements (i.e. have high sensitivity) and convert this movement most efficiently to an electrical voltage. In this paper we made an analysis of the behavior of the piezoelectric plate under the influence of the two kinds of waves - longitudinal and transversal. In the first case analyzes the response of the model against the front of the acoustic wave applied normal to the site of the piezoelectric plate that simulates the arrival of the longitudinal wave. In the second case - the response of the same model, but against the front tangential movement that simulates the arrival of transverse waves. Such an analysis is relevant, since mechanical response of the piezoelectric plate to the impact of different types of waves has not been studied.

2. Acoustic emission sensor simulation

The investigated model presented in figure 1. For Model 1 were selected physical properties of ceramics. Basic physical and mechanical characteristics for the model are as follows: elastic modulus $E = 2.2 \cdot 10^5$ MPa, the Poisson's ratio $\nu = 0.22$, density $\rho = 2.3 \cdot 10^3$ kg/m^3, wavelength $\lambda_{min} = 10$ mm, longitudinal wave velocity $C_l = 9780$ m/s.

Boundary conditions are presented in figure 1. At the edge of the lower edge of a ban on the movement of the axis *z*. Also, two nodes of edge A lying on the same diameter (nodes 21 and 221), ban the displacement along the x axis and rotations about the axes *x, y, z*. In all nodes of edge A Model 1 applied axis displacement U_z = 100 micrometers in the form of steps duration $1 \cdot 10^{-5}$ s, modeling, thus coming to the piezoceramic plates longitudinal acoustic wave (normal to the surface of the plates). The calculation is made in the FEM system COSMOS/M, module nonlinear dynamic analysis. The calculation parameters are fully compliant with the spatial and temporal sampling, detailed in [2]. These calculated results are shown in figure 2, where the fixed scale –300 ... 300 micrometers.

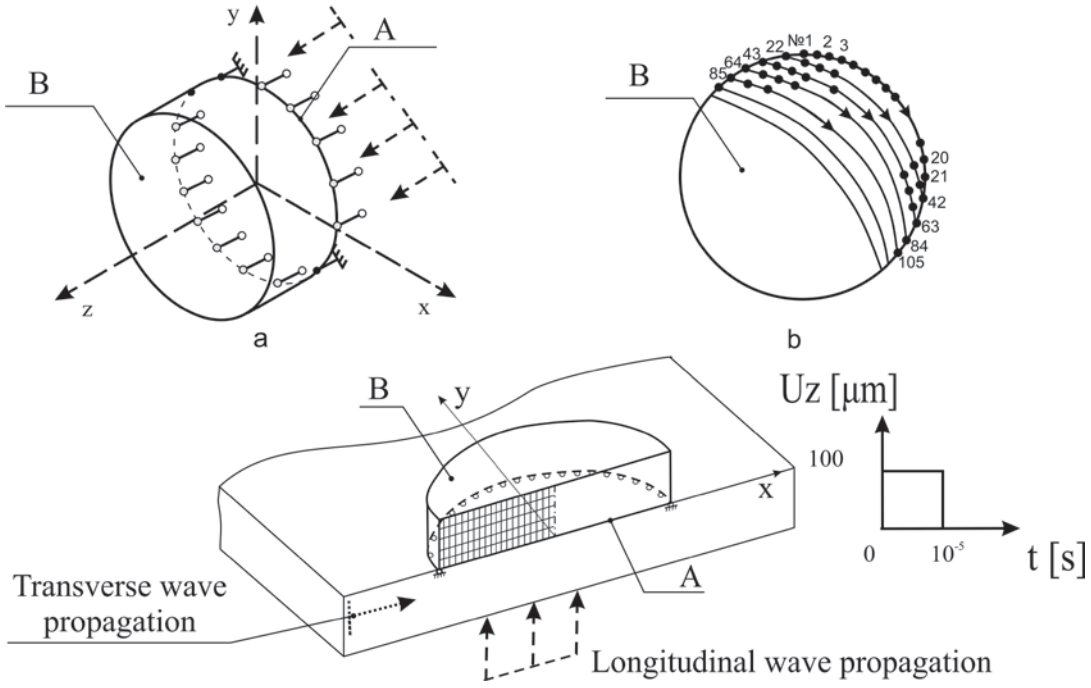

Figure 1. The FEM model of the AE sensor.

Figure 2a shows the distribution of displacements U_z of wave front extends from the edge A and reached the center of the model at time $2.5 \cdot 10^{-7}$ s. According to theoretical calculations, the arrival time of the waves on the edge B was $5 \cdot 10^{-7}$ s. Next figure 2b shows that the theoretical calculations and numerical simulation results are the same. Figure 2c observed maximum positive displacement at edge B. In the following times at $1 \cdot 10^{-6}$ s and $1.25 \cdot 10^{-6}$ s the process of reflection of the wave from the free edge B. At time $1.5 \cdot 10^{-6}$ s there are zero field displacements – the wave is reflected and passes the zero position. At time $1.75 \cdot 10^{-6}$ s we can observe negative maximum displacement of edge B. On figure 2h compression wave front moves to edge A, at time $2.25 \cdot 10^{-6}$ s reflection occurs and at time $2.5 \cdot 10^{-6}$ s the model once again has "zero" displacement. At time $2.75 \cdot 10^{-6}$ s there are observed positive movements of edge B and the process is repeated.

Thus, the arrival of the longitudinal acoustic wave on piezoelectric plate leads to demonstrated in figures 2a–p modes oscillations, the main strain is a "tension-compression". In the framework of this problem it is evident that vibrations of the plate in this fashion will result in maximum electrical signal to the piezoelectric plates, since the total deformation of the upper face at a certain time in such a fashion is maximized.

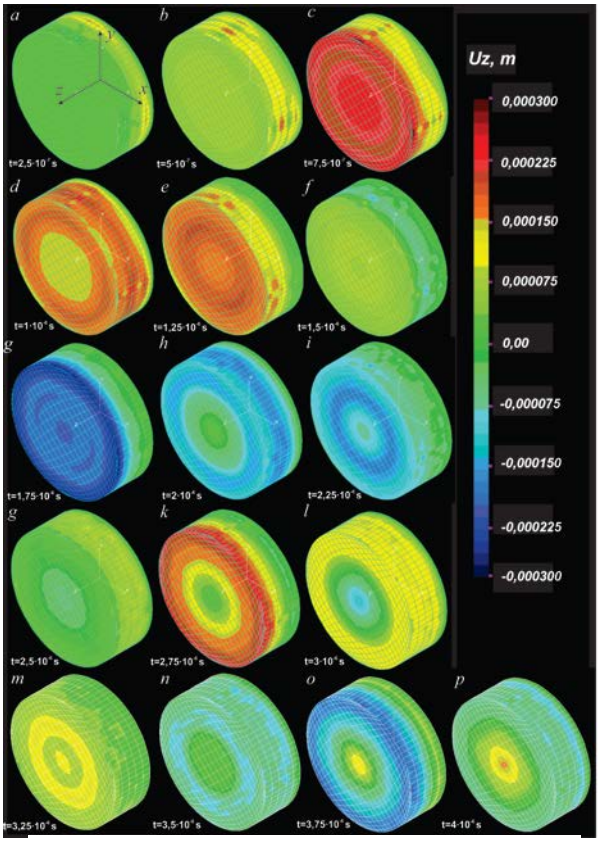

Figure 2. Displacements U_z for Model 1, with the arrival of longitudinal waves.

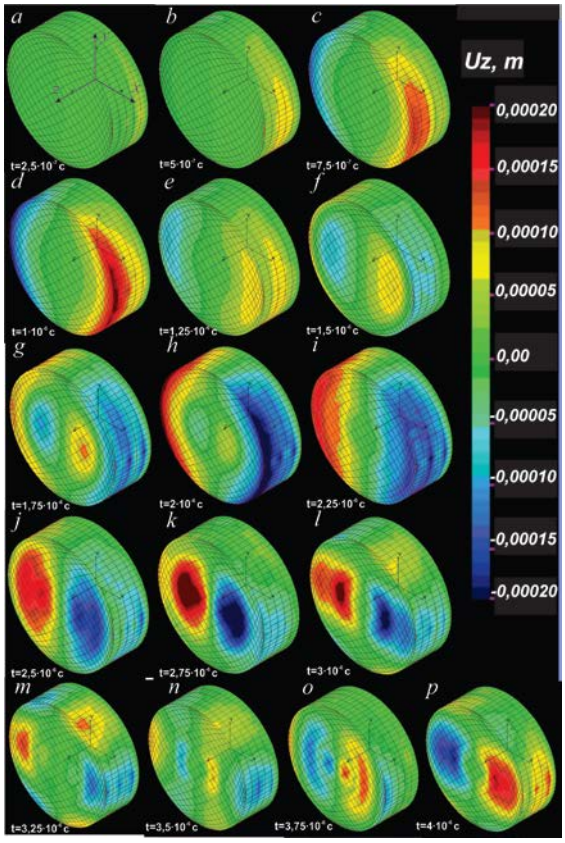

Figure 3. Displacements U_z for Model 1, with the arrival of a transverse wave.

The second experiment with the Model 1 consisted in changing the direction of perturbing displacement on the U_x. The rest of the boundary and initial conditions remain unchanged. Figure 3a-p analyzes the displacement U_z of model edge B.

On figure 3a at time $2.5 \cdot 10^{-7}$ s the wave comes from the edge A. On figure 3b the maximum wave extends to the middle of the model. On figure 3c the maximum wave comes to top face. On figure 3d the wave reaches the upper face and displacements U_z are maximized at two parts of the upper face. By the time $1.5 \cdot 10^{-6}$ s from the zone of maximum displacement shifted to the center, the diagram becomes more complex, with two-bend at time $2 \cdot 10^{-6}$ s. A maximum displacement U_z again observed at the edges, with the zone of negative (blue color) and positive (red color) movements are reversed when compared to figure 3d. Next, the positive and negative peaks of displacements are shifted again to the center of the model and the process repeats.

The results of mathematical modeling show that the oscillation mode determines the distribution of node displacements upper edge model. In real piezoelectric sensor the sputtered layer is the upper edge (the so-called electrode), where the electric potential is recorded. In the above examples the electric potential (total displacement U_z) is smaller at several orders of magnitude for the transverse waves than for longitudinal waves.

3. Experimental results

The non-destructive testing of thousands of solebars of the freight-car truck was done in 2012–2014 years. At the same time the AE sensor position during AE control significantly influences to the accuracy of the AE control. The AE sensors work more effective when their locations are in the zones of extreme displacements of the object surface. In this regard, relevant is the problem of determining such zones.

The finite element model of a solebar of the freight-car truck were drawn in the software package SOLIDWORKS. The model accounts the most important and general structural elements and the nature of cross-sections. Acoustic emission signal was simulated by force with an amplitude of 1 kN and a duration of $1 \cdot 10^{-5}$ s [3,4].

The direction of applied force is shown in figure 4a by the arrow. The highest frequency of fastest generated acoustic waves mode consists of 100 kHz. In this case, the wavelength of the propagating acoustic waves is more than 6 cm. The selection of the applied force place was based on the frequent breaks statistics. Adaptive finite element mesh generating was provided in the field of geometric concentrators (holes, fillets, casting, etc.). The finite element size in these fields were mounted 5 mm, i.e. the density of the mesh in these fields was ~ 10-12 finite elements on a single characteristic size of the wave, which is in according with the requirements of [1]. Maximum step time discretization were chosen uniform and equal to 10^{-6} s, it's were provided 10 iterations per period of the pulse duration.

The model were consisted of 133 541 nodes, 73687 elements.

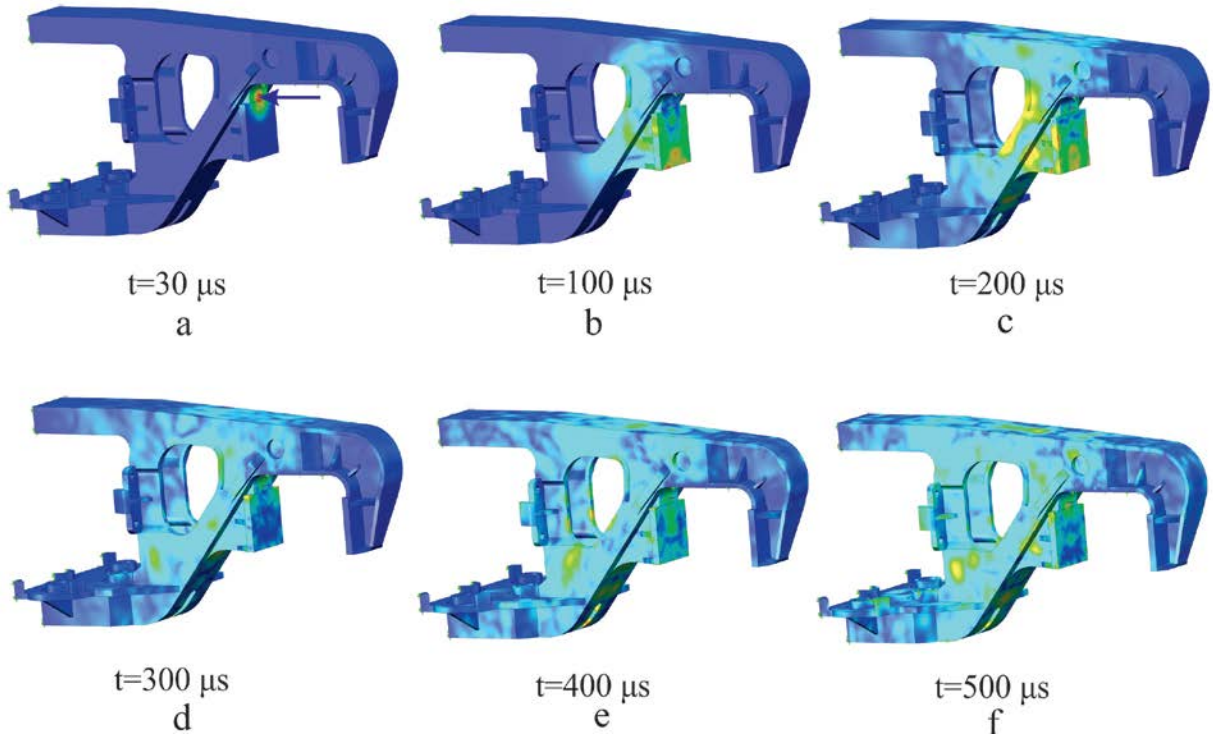

Figure 4. Wave propagation in a finite element model of solebar of the freight-car truck.

The theoretical speed of fastest generated acoustic waves mode was 5.9 mm/μs. Figure 4a – 4f shows the computing result of displacements of model surface. The node displacements are presented at time from 0 to 500 μs. According to preliminary estimates the computing acoustic wave propagates to 30 mm by 50 μs. Thus the results of numerical modeling of the acoustic wave propagation are conforming to theoretical estimates.

Figure 5 presents the regular places of AE sensors in the frontal plane *YZ* (a) and the computing results of the displacements U_x component of the solebar surface (b) at time $t=1 \cdot 10^{-3}$ s. The process is well established. The sign "+" in the figure 5b is indicated the installing places of AE sensors in accordance with existing technological instruction. The figure shows that AE sensors № 9(12), № 10(11), № 13(16) are installed on the solebar zones where the mean value of normal displacements U_x component tends to zero (green). While AE sensors are the most sensitive to the normal component of the displacements.

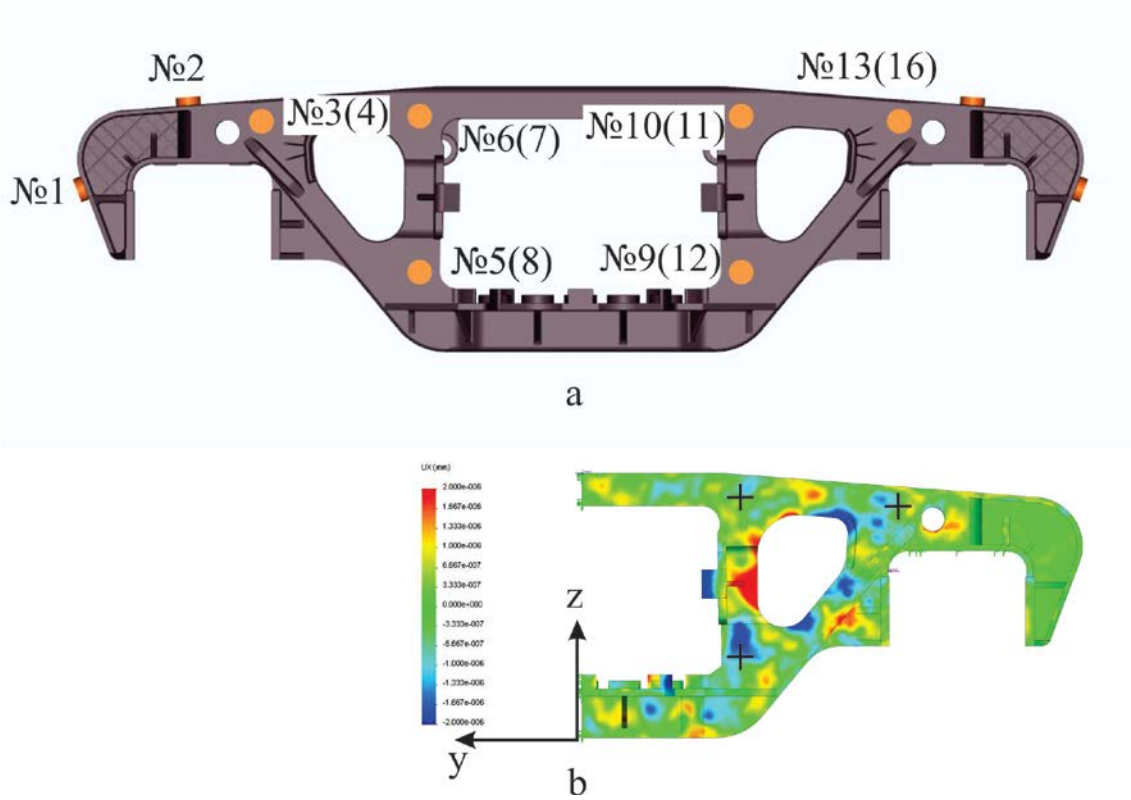

Figure 5. The installing regular places of AE sensors in accordance with existing technological instruction (a) and U_x displacements distribution at the time 0.001 s (b).

The analysis of the distributions of displacements U_x component in the finite element model allows to select nodes with high value of normal displacements (U_x component). The value of normal displacements in these nodes is significantly more than at the regular places of installation of AE sensors. The column 2 of table 1 consists the absolute value of the surface U_x displacement in the regular places of installation of AE sensors, the column 3 consists average displacements at the nodes in the zones in which it is recommended to transfer the centers sensors. Column 4 shows the ratio of values of the 2-nd and 3-rd columns.

Table 1. Computing results. Values of U_x displacements in regular and recommended places of solebar surface and its ratio

Sensors number	Normal displacements (U_x component) in the regular nodes, m, $\cdot 10^{-6}$ s	Normal displacements (U_x component) in the recommended nodes, m, $\cdot 10^{-6}$	The ratio
1	*2*	*3*	*4*
№9(12)	-1.11	-2.02	1.8
№10(11)	-0.69	-0.86	1.2
№13(16)	-0.22	-1.43	6.5

Using the finite element method the results of acoustic waves propagation in the object of complex shape were obtained. According computing results AE sensor No.9, 12 are recommended to transfer to z=41 mm; AE sensor No.10, 11 are recommended to transfer to z=26 mm and y=-26.5 mm; AE sensor No.13, 16 are recommended to transfer to y=49 mm, and z=2 mm.

The physical experiment was carried out for comparison of computing and nature results. The experiment includes the first case, the AE sensors were installed in the regular places, the second case, the AE sensors were installed in the recommended places.

The acoustic emission signals were generated by pencil-lead breaks. The experimentally, place of application of force was equivalently to the numerical experiment condition. The system and channels setup were made according to the existing technological instruction. Pencil-lead breaks are widely used as a reproducible source for test signals in acoustic emission applications (Hsu-Nielsen source) [5,6].

To analyze the influence of transferring the sensor installing places were taken 20 series of breaks for the first and second experiment cases. We analyzed the amplitude of the signals. The experimental results were shown the increasing the average level of experimental signals with comparing of the first and second experiment.

4. References

[1] Nasedkin A V, Shikhman V M and Zakharova S V (2011) Finite-element calculation of high-temperature acoustic-emission transducers *Russian Journal of Nondestructive Testing* **47**(7) 468–479

[2] Sych T, Gerasimov S and Kuleshov V (2012) Simulation of the propagation of acoustic waves by the finite element method *Russian journal of nondestructive testing* **48**(3) 147–152

[3] Hora P and Cerneva O (2010) Acoustic emission source modeling *Applied and Computational Mechanics* **4** 25–36

[4] Markus G and Richler S (2015) Finite element modeling of cracks as acoustic emission sources *Journal of nondestructive evaluation* **34** 4–17

[5] Hamstad M (2007) Acoustic emission source location in a thick steel plate by Lamb modes *Journal of acoustic emissio*n **25** 194–214

[6] Wotzka D, Boczar T and Fracz P (2011) Mathematical model and numerical analysis of AE wave generated by partial discharges *Optical and acoustical methods in science and technology* **120**(4) 767–771